

# A microanalytical study of the early stages of recrystallization in the nickel-base superalloy APK1

P. R. HOWELL

*Department of Materials Science and Engineering, The Pennsylvania State University, University Park, Pennsylvania, USA*

J. V. BEE

*Department of Chemical Engineering, Adelaide University, South Australia*

Analytical electron microscopy has been used to investigate the composition of various microstructural features in a powder-produced nickel-base superalloy. Specifically, it is shown that in the early stages of recrystallization the strain-free grains are depleted in the  $\gamma'$ -forming elements (i.e. titanium and aluminium). This observation is consistent with the hypothesis that recrystallization in this alloy is initiated in the immediate vicinity of large intergranular  $\gamma'$  particles. It is also shown that the composition of  $\gamma'$  can be written as  $(\text{Ni}, \text{Co})_3 (\text{Al}, \text{Ti}, \text{Cr})$ .

## 1. Introduction

A number of studies have been reported concerning the recrystallization of powder-produced nickel-base superalloys (e.g. [1-3]) and a number of nucleation sites have been proposed, e.g. large carbides [4], large  $\gamma'$  precipitates [5] and large  $\gamma'$  precipitates at grain boundaries [1]. In this study, analytical electron microscopy (AEM) has been used to document the early stage of the recrystallization process and to determine the composition of various microstructural components, using energy-dispersive X-ray spectrometry (EDS). It has been found that the first-formed strain-free grains are depleted in both aluminium and titanium (the  $\gamma'$ -forming elements), which is consistent with the hypothesis [2] that these grains form in contact with large intergranular precipitates. It is also found that the  $\gamma'$  phase is based on the composition  $(\text{Ni}, \text{Co})_3 (\text{Al}, \text{Ti}, \text{Cr})$  which correlates well with a number of other studies using EDS in the AEM [6] and atom-probe microanalysis [7-9].

## 2. Experimental procedure

The alloy investigated had the following nominal composition (at %):

| Cr   | Mo  | Ti  | Ni   | Co   | Al  | C    |
|------|-----|-----|------|------|-----|------|
| 16.6 | 3.1 | 4.2 | 52.1 | 15.6 | 8.3 | 0.03 |

The material had been hot-isostatically pressed (HIPed) above the  $\gamma'$  solvus. Subsequently, the alloy was isothermally-hot forged at 1323 K to 66% reduction in height and air-cooled.

Specimens, of both the HIPed and forged materials, for transmission electron microscopy, were prepared using standard techniques [2] and examined in either a Jeol 200 CX operating at 200 kV or a Philips EM 400T operating at 120 kV. Quantitative EDS microanalysis employed the Link systems RTS-2/FLS computer

program which compares peak shapes with those of standard spectra of pure elemental standards, and applies a thin-foil approximation [10] with corrections for absorption.  $\gamma'$  compositions were determined from particles whose dimensions ( $\sim 500$  nm diameter) were large compared with the foil thickness ( $\sim 100$  nm). This ensured that the matrix contribution to the spectrum was minimal. The estimated statistical error in composition for all the elements analysed was less than 1%.

## 3. Results and discussion

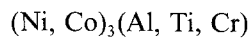
Fig. 1 is a centred dark-field micrograph of the as-HIPed specimen material. Essentially, the slow cooling from the HIPing temperature leads to the development of a relatively uniform dispersion of cuboidal  $\gamma'$ , together with a fine dispersion of  $\gamma'$  in the intercuboidal regions. In addition, the  $\gamma$ - $\gamma'$  grain boundaries were decorated with a dispersion of massive  $\gamma'$  precipitates and a  $\gamma'$ -depleted zone invariably developed at the  $\gamma$ - $\gamma'$  grain boundaries (see also Fig. 1 of [2]).

The composition of the alloy was investigated using an area scan in the scanning transmission (STEM) mode and the results of this analysis are presented in Table I. As can be seen, good agreement is obtained between the nominal composition and that determined by STEM EDS. The compositions of the matrix and the cuboidal  $\gamma'$  were also investigated using a fine STEM probe ( $\sim 10$  nm diameter), and typical analyses of both microstructural features are also given in Table I. The  $\gamma'$  is enriched in aluminium and titanium and depleted in both cobalt and chromium. Conversely, the  $\gamma$  matrix is enriched in cobalt and chromium whilst being deficient in the  $\gamma'$ -forming elements (i.e. aluminium and titanium). The significant aluminium and titanium levels observed in the matrix are due to the

TABLE I Compositions of phases

| Phase                     | Composition (at %) |      |     |      |      |     |
|---------------------------|--------------------|------|-----|------|------|-----|
|                           | Ni                 | Al   | Ti  | Cr   | Co   | Mo  |
| Alloy nominal composition | 52.1               | 8.3  | 4.2 | 16.6 | 15.6 | 3.1 |
| Alloy composition by STEM | 51.3               | 8.7  | 4.1 | 14.9 | 16.4 | 4.6 |
| Matrix $\gamma$           | 47.2               | 4.3  | 1.7 | 22.6 | 19.9 | 4.3 |
| Cuboidal $\gamma'$        | 63.5               | 13.5 | 9.4 | 3.4  | 9.5  | 0.6 |
| Recrystallized grains     | 50.1               | 3.5  | 2.4 | 20.4 | 20.6 | 3.0 |

fact that the matrix contains a fine spherical dispersion of  $\gamma'$  (Fig. 1) which is impossible to exclude from the analysis. Significant variations in both the aluminium and titanium contents of  $\gamma'$  were observed from precipitate to precipitate. However, the average levels of these elements strongly suggest that the composition of the  $\gamma'$  can be written as follows:



where the chromium level remains fairly constant at  $\sim 3\%$ . This composition is consistent with those determined using atom-probe field-ion microscopy, both on a similar alloy [11] and in other nickel-base superalloys [7, 9].

The effect of hot isothermal forging is to impart a large degree of warm work to the matrix, and the large  $\gamma'$  precipitates adopt degenerate morphologies as illustrated in Fig. 2. However, in regions close to the original grain boundaries, small recrystallized grains were observed. Fig. 3 is a bright-field micrograph of a grain boundary region. The large intergranular  $\gamma'$  precipitate has polygonized to form two sub-grains A and B. A recrystallized grain (C) is seen in association with the large intergranular  $\gamma'$  precipitate. This recrystallized grain contains an annealing twin (arrowed) and a dispersion of fine, approximately spherical  $\gamma'$  precipitates. These precipitates have diameters in the range 70 to 170 nm. In comparison, the intragranular  $\gamma'$  precipitates, in both the HIPed material and in the body of the hot-worked grains, were approximately  $0.5 \mu\text{m}$  in diameter (see also Figs 1 and 2). Figs 4a and b are bright-field and  $\gamma'$ -centred dark-field micro-

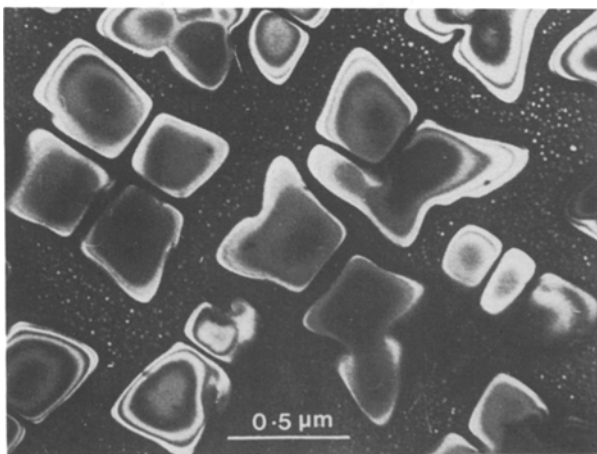


Figure 1  $\gamma'$ -centred dark-field micrograph of the HIPed specimen material.

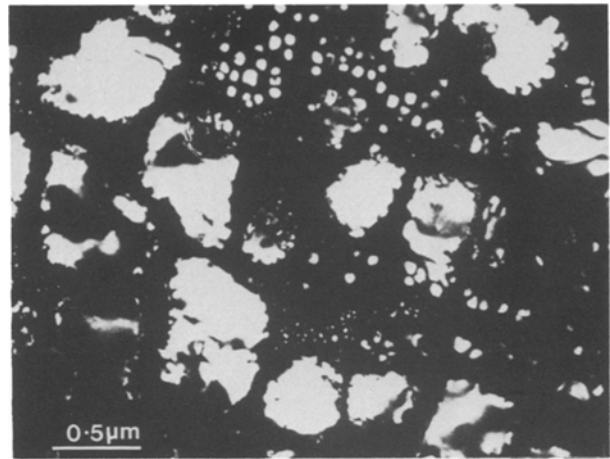


Figure 2  $\gamma'$ -centred dark-field micrograph of a warm-worked grain in the forged specimen material.

graphs, respectively, of another recrystallized region. In common with Fig. 3, large intergranular precipitates are present (Fig. 4a). The recrystallized grain contains spherical/cuboidal  $\gamma'$  ( $\sim 50 \text{ nm}$  diameter) together with a much finer dispersion of cooling  $\gamma'$  and larger, more irregular  $\gamma'$  (marked "c"). The precipitates marked "b" in Figs 4a and b originate from the hot-worked unrecrystallized regions. Finally, Fig. 5 is a  $\gamma'$ -centred dark-field micrograph of a recrystallized grain and a low number density of spherical/cuboidal precipitates ( $\sim 35 \text{ nm}$  in diameter) are observed.

In previous studies [1, 2], it was shown that the major reactions occurring during the later stages of recrystallization were

(i) dissolution of the degenerate  $\gamma'$  precipitates (Fig. 2) at the advancing interface and a concomitant re-precipitation at the interface to produce a discontinuous  $\gamma$ - $\gamma'$  colony; and

(ii) selective coarsening of  $\gamma'$ , from the hot-worked regions, at the recrystallization interface to produce a duplex  $\gamma$ - $\gamma'$  structure.

However, reference to Figs 3 to 5 shows that the dominant reaction which is occurring, during the early stages of recrystallization, is dissolution of the degenerate  $\gamma'$  at the interface followed by re-precipitation of  $\gamma'$  behind the interface within the recrystallized

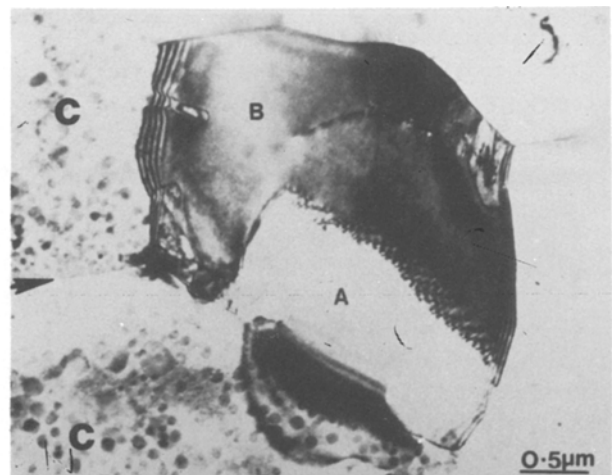


Figure 3 Bright-field micrograph of a recrystallized grain (C) in contact with a large intergranular  $\gamma'$  precipitate.

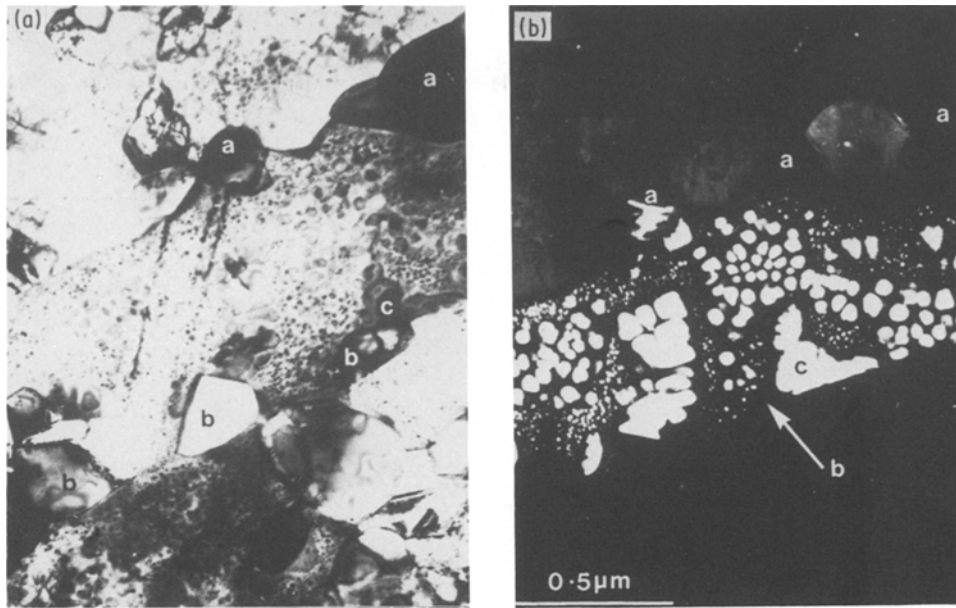


Figure 4 (a) Bright-field and (b)  $\gamma'$ -centred dark-field micrographs of a recrystallized grain.

grains.\* This observation lends strong support to the contention that the recrystallized grains form in the vicinity of the prior grain boundaries, since it is known [12, 13] that a low supersaturation of the  $\gamma'$ -forming elements tends to promote dissolution at the advancing interface and subsequent re-precipitation within the recrystallized volume. However, this mechanism requires the recrystallized grains to be deficient in aluminium and titanium, and although this may be inferred from the low volume fraction of  $\gamma'$  present in Fig. 5 and the association between the recrystallized grain and the massive  $\gamma'$  precipitate in Fig. 3, no apparent association between the recrystallized grains and grain-boundary  $\gamma'$  was often observed due to sectioning effects in the thin foils.

However, area-scan analyses of the recrystallized grains showed that in all cases they were depleted in both aluminium and titanium and a "typical" composition of a recrystallized grain is given in Table I. It should be appreciated that there was a large scatter in

composition from grain to grain and this is reflected in the variations in the volume fraction of  $\gamma'$ , within individual recrystallized grains, which may be gauged with reference to Figs 3 to 5. However, the general trends are

(i) the aluminium and titanium levels are always lower than that characteristic of the bulk, and in certain cases are not much different than those of the  $\gamma$  matrix; and

(ii) the cobalt and chromium levels are much higher than the bulk level and often approach those of the  $\gamma$  matrix.

#### 4. Summary

The microstructural and microanalytical results show that recrystallization is initiated in the  $\gamma'$ -depleted regions which are located in the vicinity of the large intergranular  $\gamma'$  precipitates. These first-formed strain-free grains contain a dispersion of spherical/cuboidal  $\gamma'$  precipitates which are typically less than 200 nm in diameter. In comparison, continued recrystallization into the warm-worked regions either produces discontinuous  $\gamma$ - $\gamma'$  colonies or duplex  $\gamma$ - $\gamma'$  regions.

#### References

1. J. V. BEE, A. R. JONES and P. R. HOWELL, in Proceedings of Conference on Recrystallization and Grain Growth of Multi-Phase and Particle-Containing Materials, Risø, Roskilde, Denmark 1980 (Risø National Laboratory, 1980) p. 153.
2. *Idem*, *J. Mater. Sci.* **15** (1980) 337.
3. A. J. PORTER and B. RALPH, in Proceedings of Conference on Recrystallization and Grain Growth of Multi-Phase and Particle-Containing Materials, Risø, 1980 (Risø National Laboratory, 1980) p. 147.
4. L. WINBERG and M. DAHLEN, *J. Mater. Sci.* **13** (1978) 2365.
5. S. DERMARKER and J. L. STRUDEL, in Proceedings of Conference on Recrystallization and Grain Growth of

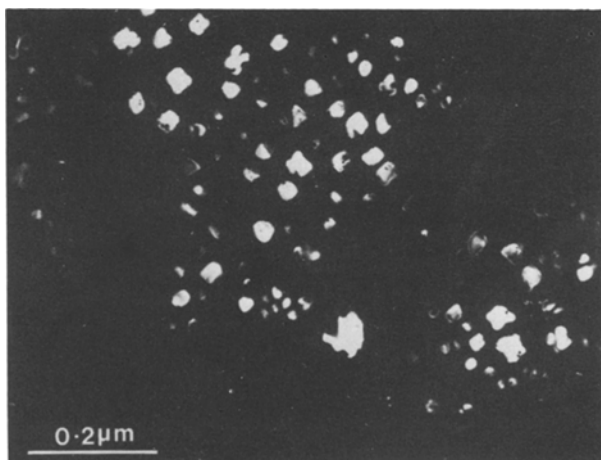


Figure 5  $\gamma'$ -centred dark-field image of a recrystallized grain.

\*It is interesting to note that in certain instances the onset of a discontinuous reaction was observed. For example the large irregular precipitates (e.g. "c" in Fig. 4b) are in contact with the interface, and continued growth will lead to the development of a discontinuous colony.

- Multi-Phase and Particle-Containing Materials, Risø, 1980 (Risø National Laboratory, 1980) p. 139.
6. M. P. SHAW, R. C. ECOB, A. J. PORTER and B. RALPH, in Proceedings of Conference on Quantitative Microanalysis with High Spatial Resolution, UMIST, Manchester, 1981 (The Metals Society, London, 1981) p. 229.
  7. P. A. BEAVEN, M. K. MILLER and G. D. W. SMITH, *Inst. Phys. Conf. Ser.* No. 36 (1977) 199.
  8. J. V. WOOD, P. F. MILLS, J. K. BINGHAM and J. V. BEE, *Met. Trans. A* **10A** (1979) 575.
  9. K. N. DELARGY and G. D. W. SMITH, *ibid.* **14A** (1983) 1771.
  10. G. CLIFF and G. W. LORIMER, *J. Microsc.* **103** (1975) 203.
  11. J. V. WOOD, P. F. MILLS, A. R. WAUGH and J. V. BEE, *J. Mater. Sci.* **15** (1980) 2709.
  12. B. RALPH, C. BARLOW, B. COOKE and A. PORTER, in Proceedings of Conference on Recrystallization and Grain Growth of Multi-Phase and Particle-Containing Materials, Risø, 1980 (Risø National Laboratory, 1980) p. 229.
  13. E. GRANT, A. PORTER and B. RALPH, *J. Mater. Sci.* **19** (1984) 3554.

*Received 2 June  
and accepted 27 July 1987*